MINISTRY OF EDUCATION AND SCIENCE OF UKRAINE
KYIV NATIONAL UNIVERSITY OF TECHNOLOGIES AND DESIGN
Faculty of Chemical and Biopharmaceutical Technologies
Department of Biotechnology, Leather and Fur

QUALIFICATION THESIS

on the topic **Study on the effect of TiO_2 Crystal morphology on its antibacterial activity**
First (Bachelor's) level of higher education
Specialty 162 "Biotechnology and Bioengineering"
Educational and professional program "Biotechnology"

Completed: student of group
BEBT-21
Xie Xiaoyun
Scientific supervisor
Olena Okhmat, Ph.D., Assoc. Prof.
Reviewer
Iryna Voloshyna, Ph.D., Assoc. Prof.

Kyiv 2025

KYIV NATIONAL UNIVERSITY OF TECHNOLOGIES AND DESIGN

Faculty: Chemical and Biopharmaceutical Technologies
Department: Biotechnology, Leather and Fur
First (Bachelor's) level of higher education
Specialty: 162 Biotechnology and Bioengineering
Educational and professional program Biotechnology

APPROVE
Head of Biotechnology, Leather and Fur Department, Professor,
Dr. Sc., Prof.
___________Olena MOKROUSOVA
«___»_______________2025

ASSIGNMENTS
FOR THE QUALIFICATION THESIS
Xie Xiaoyun

1. Thesis topic **Study on the effect of TiO_2 Crystal morphology on its antibacterial activity**

Scientific supervisor Ph.D., Asos. Prof. Olena OKHMAT

approved by the order of KNUTD “05” March 2025, № 50-уч

2. Initial data for work: assignments for qualification thesis, scientific literature on the topic of qualification thesis, materials of Pre-graduation practice

3. Content of the thesis (list of questions to be developed): literature review; object, purpose, and methods of the study; experimental part; conclusions

4. Date of issuance of the assignments 05.03.2025

WORK CALENDAR

№	The name of the stages of the qualification thesis	Terms of performance of stage	Note on performance
1	Introduction	until 11 April 2025	
2	Chapter 1. Literature review	until 20 April 2025	
3	Chapter 2. Object, purpose, and methods of the study	until 30 April 2025	
4	Chapter 3. Experimental part	until 11 May 2025	
5	Conclusions	until 15 May 2025	
6	Draw up a bachelor's thesis (final version)	until 25 May 2025	
7	Submission of qualification work to the supervisor for feedback	until 27 May 2025	
8	Submission of bachelor's thesis to the department for review (14 days before the defense)	28 May 2025	
9	Checking the bachelor's thesis for signs of plagiarism (10 days before the defense)		Similarity coefficient ____% Citation rate ____%
10	Submission of bachelor's thesis for approval by the head of the department (from 7 days before the defense)		

I am familiar with the task:

Student _____________ Xie Xiaoyun

Scientific supervisor _____________ Olena OKHMAT

Abstract

Xie Xiaoyun. Study on the effect of TiO_2 Crystal morphology on its antibacterial activity. – Manuscript.

Qualification thesis on the specialty 162 «Biotechnology and Bioengineering». – Kyiv National University of Technologies and Design, Kyiv, 2025.

As an important inorganic functional material, nano-titanium dioxide (TiO_2) has attracted extensive attention due to its excellent physicochemical properties. This material not only exhibits characteristics such as non-toxicity, high chemical stability, and remarkable photoelectric conversion efficiency but also demonstrates outstanding photocatalytic performance. Based on these properties, TiO_2 nanomaterials show broad application prospects in environmental remediation and health protection, particularly in wastewater treatment, air purification, and microbial inhibition, where they hold significant value. In the field of antibacterial materials research, TiO_2 photocatalytic antibacterial agents have become a research hotspot due to their unique advantages. These materials possess high catalytic activity, excellent thermal stability, long-lasting antibacterial effects, as well as low cost and safe usage. Currently, they are recognized as one of the most promising catalytic antibacterial agents. This study employs a hydrothermal synthesis method to prepare nano-TiO_2 materials and systematically investigates the differences in antibacterial performance among various crystal structures. Using titanium sulfate as the precursor, a series of samples were prepared by controlling synthesis conditions. Multiple characterization techniques, including X-ray diffraction

(XRD), scanning electron microscopy (SEM), were utilized for comprehensive material analysis. The study focuses on exploring the structure-activity relationship between crystal structure characteristics and antibacterial performance. Additionally, comparative experiments under light and dark conditions were designed to evaluate the differences in antibacterial activity among different TiO_2 crystal phases.

Key words: TiO_2, Antibacterial activity, Hydrothermal method, Crystalline form, anatase, brookite

TABLE OF CONTENTS

INTRODUCTION

This thesis, investigates the relationship between the crystal structure of titanium dioxide (TiO_2) and its antibacterial performance. The research focuses on the differences in antibacterial activity among anatase, brookite, and mixed-phase TiO_2, synthesized via a hydrothermal method using titanium sulfate as the precursor.

Key aspects of the study include:

1. Material Preparation and Characterization: TiO_2 nanoparticles were synthesized under controlled conditions and analyzed using X-ray diffraction (XRD), scanning electron microscopy (SEM), and ultraviolet-visible spectroscopy (UV-Vis) to determine their crystal phases, morphologies, and optical properties.

2. Antibacterial Performance: The antibacterial activities of the TiO_2 samples were evaluated against *Escherichia coli* under both light and dark conditions. Results demonstrated that anatase-phase TiO_2 exhibited superior photocatalytic antibacterial activity under light exposure, while no significant antibacterial effect was observed in the dark.

3. Findings and Implications: The study highlights the critical role of crystal morphology in TiO_2's antibacterial efficiency, with anatase showing the highest performance due to its optimal bandgap and surface properties. The research provides valuable insights for designing TiO_2-based antibacterial materials for applications in healthcare, environmental remediation, and food packaging.

This work contributes to the understanding of structure-activity relationships in photocatalytic materials and offers practical guidance for developing advanced antibacterial agents.

CHAPTER 1
LITERATURE REVIEW

1.1 Purpose and significance of the topic selection

1.1.1 Research background

Nano titanium dioxide (TiO_2) is a photocatalytic antibacterial agent [1]. It has a high surface energy and good antibacterial effect, and is widely used in medical treatment, food packaging, sewage treatment and other fields [2]. Studies have shown that TiO_2 has a good antibacterial effect on bacteria, fungi and molds. However, its antibacterial activity is significantly affected by the crystal form (such as anatase, plate titanite). Anatase-type TiO_2, due to its narrow band gap, can efficiently generate reactive oxygen species and destroy the microbial structure under ultraviolet light. The rutile type has a relatively low antibacterial efficiency due to the high recombination rate of photogenerated carriers [3]. Clarifying the influence of different crystal forms on antibacterial properties is of great significance for the development of efficient antibacterial materials.

1.1.2 Research objectives and significance

This study aims to systematically compare the antibacterial activities of different crystal forms of TiO_2, reveal the correlation between crystal forms and antibacterial efficiency, and provide a theoretical basis for optimizing the crystal form design of TiO_2-based antibacterial materials. The research results have extensive applications in fields such as medical equipment, water treatment, and food packaging, which is conducive to solving the problem of drug-resistant bacterial infections[4] and has significant scientific value and social significance.

1.2 Research status and applications at home and abroad

1.2.1 Domestic research progress

In 2015, the team led by Xie Yuan from Southwest Jiaotong University prepared silver-loaded nano-tio(Ag/TiO_2) by heating and decomposing silver-containing precursors. According to the research, under the condition of no light, the silver-loaded TiO_2 significantly enhances the antibacterial activity through the release of Ag^+ , and the diameter of the inhibition ring reaches 1.57 cm. This research provides a new idea for the antibacterial application of TiO_2 in the absence of light. Another study by Xie Yuan's team optimized the preparation process of Ag/TiO_2. Through SEM and XRD characterization, it was found that Ag was uniformly deposited on the surface of TiO_2, significantly enhancing the antibacterial performance in the absence of light, providing technical support for the development of medical device coatings. In 2020, the team led by Hu Yingying from Northeast Agricultural University studied the antibacterial mechanism of nano-tio_2 photocatalytic technology and its application in food packaging. Research indicates that TiO_2 under ultraviolet light destroys bacterial cell membranes by generating reactive oxygen species, and has demonstrated its potential in food surface disinfection and packaging materials [5]. In 2018, domestic scholar Wu Ying prepared spindle-shaped composite nano TiO_2 by sol-gel method and found that the antibacterial rate of anatase-type TiO_2 against Escherichia coli could reach 65%, and the antibacterial performance was further improved after doping with Cu ions. Emphasis is placed on the synergistic effect between crystal form regulation and metal doping [4].

1.2.2 Research progress abroad

In 2020, a review published in ACS Nano of the United States pointed out that anatase-type TiO_2 is more prone to generating reactive oxygen species due to the high density of hydroxyl groups on its surface, while rutile type has limited antibacterial activity due to the high electron-hole recombination rate. This study provides a theoretical basis for crystal form selection [6]. In 2024, a Canadian team developed TiO_2 composites modified by reduced graphene oxide (rGO). Experiments show that the antibacterial rate of rGO-TiO_2 against Enterobacter hormaechei under visible light has increased to 90%, attributed to the enhanced separation efficiency of photogenerated carriers and the physical destruction of the bacterial cell wall [6]. In 2019, Japanese scholars reported in the "Journal of Materials Chemistry" that by synthesizing the mixed crystal type TiO_2 (anatase/rutile) through the hydrothermal method, it was found that the mixed crystal structure could broaden the range of light absorption and increase the antibacterial efficiency under visible light by 40%. The study emphasizes the regulatory effect of crystal form ratio on photocatalytic performance [5]. In 2015, a study by Degaussa of Germany based on P25-type TiO_2 (anatase/rutiite mixed phase) showed that its photocatalytic activity had an inactivation rate of over 80% against Staphylococcus aureus under ultraviolet light. This achievement has promoted the commercial application of TiO_2 in the field of antibacterial coatings. In 2020, the European joint research group published a study in "Applied Catalysis B: Environmental". By doping anatase-type TiO_2 with Fe^{3+}, the light response range was extended to the visible light region, and it was proved that the generation of ROS after doping increased by 1.5 times, significantly enhancing the inhibitory effect on fungi.

In addition, for the preparation method of TiO_2 photocatalyst, Tian and Hidalgo utilized the photochemical deposition method. Among them, Tian et al. deposited smaller-sized Pd clusters on TiO_2 nanowires by photoreduction method [7]. Hidalgo et al. regulated the size of Au nanoparticles deposited on the TiO_2 surface by controlling conditions such as light intensity, light exposure time, and the content of metal precursors. They found that small-sized Au nanoparticles could be successfully synthesized on the TiO_2 surface with a small amount of metal precursor solution under the action of low light intensity and short light exposure time [8]. Han et al. first successfully prepared spindle-shaped nanoporous anatase-type TiO_2 (101) mesoTiO_2 by the hydrothermal method, and then used the depositation-precipitation method to load Au nanoparticles onto meso TiO_2 to form Aux/meso TiO_2. It was found that Au nanoparticles were highly dispersed on the surface of meso TiO_2 to obtain the Aux/meso TiO_2 photocatalyst. A tight Schottky junction was established between Au nanoparticles and mesoTiO_2, which improved its photocatalytic activity and stability [9]. Wrasman et al. first synthesized the Pd/Au double alloy colloid by the sol-gel method and then loaded it onto the TiO_2 surface. The catalytic activity and selectivity of the obtained catalyst Pd/Au/

TiO_2 were regulated by changing and adjusting the surface composition of Pd/Au alloy nanocrystals [10]. Zhou et al. made a breakthrough in the atomic layer deposition method. Zhou et al. used methylcyclopentadienyl -(trimethyl) platinum (IV) and oxygen as precursors and deposited platinum (Pt) on the surface of TiO_2 photocatalyst nanoparticles by the ALD method. They also investigated the effect of deposition temperature (150 ° C - 400 ° C) on the deposition of Pt nanoparticles. The results show that at the deposition temperature of 320 ° C, conducting a Pt ALD cycle can maximize the surface dispersion of Pt nanoparticles and improve the performance of TiO_2 nano-photocatalysts by three times [11].

1.2.3 Applications of titanium dioxide in antibacterial properties

With the continuous development and utilization of the antibacterial properties of nano-tio_2 photocatalysts by people, antibacterial ceramics, antibacterial plastics, antibacterial coatings, antibacterial fibers and antibacterial daily necessities have emerged one after another.

To expand the application potential of TiO_2 photocatalytic materials in weak light environments, researchers are dedicated to developing low-light-dependent antibacterial ceramics. Liu Ping[12] studied a self-cleaning ceramic material modified with nano-tio_2 films, which could achieve an inactivation rate of over 80% against Staphylococcus aureus in just 15 minutes under completely light-free conditions. Qian Hong's research [13] indicates that the TiO_2 antibacterial ceramics prepared by a special process can achieve a killing efficiency of up to 85% against *Staphylococcus aureus* under the irradiation of ordinary fluorescent lamps, demonstrating good practical application value. These achievements provide important technical support for the application of TiO_2 -based antibacterial materials in indoor environments.

Nano TiO_2, as an efficient photocatalytic material, can be compounded with polymer resins to prepare functional antibacterial plastics, showing significant application potential in the field of environmental purification. Studies have shown that the TiO_2/ polymer composite material developed by Xu Ruifen's[14] team exhibits excellent inhibitory effects on a variety of pathogenic microorganisms. The antibacterial test data indicate that after 24 hours of action, the inactivation efficiency against Escherichia coli, Staphylococcus aureus, and Bacillus subtilis all exceed 97%. In addition, Ding Xingeng[15] and other scholars modified polyethylene matrix with Ag-TiO_2 nanoparticles and successfully prepared antibacterial packaging films with preservation functions. Experiments confirmed that this material could extend the shelf life of fresh milk to 10 days in a 4 ° C refrigeration environment, significantly improving the safety performance of food packaging.

Nano TiO_2, as an efficient photocatalytic material, can significantly enhance the antibacterial performance when compounded with conventional coatings, and has important application value in the development of environmentally friendly functional materials. Studies show that by dispersing nano-tio_2 in the coating matrix, composite coatings with long-lasting and broad-spectrum bactericidal properties can be prepared. The TiO_2 modified coating system developed by Xu Ruifen's[16] team demonstrated excellent antibacterial activity under various light conditions. Experimental data showed that this material not only had a significant bactericidal effect under strong light conditions, but also maintained a high microbial inhibition efficiency in low-light environments (such as indoor natural light or artificial light sources) and even in the dark. This characteristic of wide light response range and strong environmental adaptability gives it significant advantages in practical applications, providing technical support for the industrial promotion of antibacterial coatings.

The coating of nano-tio$_2$ films on the surface of stainless steel can prepare stainless steel with bactericidal properties, which has broad application prospects in the food industry, medical and health care, and even ordinary households. Wang Ming[17] prepared antibacterial stainless steel coated with Ag^+/TiO_2 film. Compared with ordinary stainless steel, it has excellent corrosion resistance, improved wear resistance, and other indicators are basically the same. The bactericidal experiment on Escherichia coli found that its antibacterial performance improved with the increase of silver content in the film layer. When the silver content was greater than 2% (by mass fraction), the antibacterial rate of stainless steel could reach over 90%.

Nano TiO_2 films are loaded onto the surface of glass and can be made into glass products with sterilization functions, which can be widely used in large public places such as hospitals and hotels. The TiO_2 microcrystalline film glass prepared by Lei Yanying[18] has the characteristics of broad-spectrum and highly efficient sterilization. After being exposed to natural light for 30 minutes, the sterilization rates of *Escherichia coli*, *Staphylococcus aureus* and *Candida albicans* all reached more than 90%.

1.3 Crystal structure and physicochemical properties of titanium dioxide

1.3.1 Crystal structure

Titanium dioxide (TiO_2), as an important functional material, has three main crystal structure variants: anatase, rutile and brookite. These three crystal phases show significant differences in crystallographic characteristics and physicochemical properties.

Anatase belongs to the tetragonal crystal system (space group $I4_1/amd$), and its structural feature is that each [TiO_2] octahedron is connected to eight adjacent octahedrons by four common edges and four common vertices. Its unit cell is composed of four TiO_2 molecules and has a high electron mobility and a low dielectric constant. Therefore, it shows excellent performance in the field of photocatalysis (especially under ultraviolet light excitation conditions) and dye-sensitized solar cells.

Rutile phase also belongs to the tetragonal crystal system (space group $P4_1/mnm$), but its coordination environment is different from that of anatase: Ti atoms are located at the center of the lattice, and six oxygen atoms form an octahedral coordination. Each [TiO_2] octahedron is connected to 10 surrounding octahedrons, 8 of which are shared by vertex and 2 by edge. The unit cell of rutile contains only two TiO_2 molecules[20], and it has the highest thermodynamic stability, being the most stable crystal phase at normal temperature and pressure. Due to its relatively low catalytic activity, rutile phase is mainly used as a white pigment in coatings, plastics and cosmetics.

The perovskite phase belongs to the orhombic crystal system, and the unit cell contains six TiO_2 molecules. This crystal phase is relatively rare in nature and is prone to transform into rutile phase under heating conditions.

Rutile phase is the most stable form among the three crystal phases. Rutile and anatase undergo irreversible phase transformation during high-temperature heat treatment and are accompanied by heat release to transform into rutile structures. This phase transformation behavior has a significant impact on applications in fields such as photocatalysis and photovoltaic devices. Therefore, during the material preparation process, the heat treatment conditions need to be strictly controlled to maintain the target crystal phase.

1.3.2 Physical and chemical properties

Titanium dioxide (TiO_2), as an important functional material, has three main crystal structure variants: anatase, rutile and brookite. These three crystal phases show significant differences in crystallographic characteristics and physicochemical properties.

Anatase belongs to the tetragonal crystal system (space group $I4_1/amd$), and its structural feature is that each [TiO_2] octahedron is connected to eight adjacent octahedrons by four common edges and four common vertices. Its unit cell is composed of four TiO_2 molecules and has a high electron mobility and a low dielectric constant. Therefore, it shows excellent performance in the field of photocatalysis (especially under ultraviolet light excitation conditions) and dye-sensitized solar cells.

Rutile phase also belongs to the tetragonal crystal system (space group $P4_2$ /mnm), but its coordination environment is different from that of anatase: Ti atoms are located at the center of the lattice, and six oxygen atoms form an octahedral coordination. Each [TiO_2] octahedron is connected to 10 surrounding octahedrons, 8 of which are shared by vertex and 2 by edge. The unit cell of rutile contains only two TiO_2 molecules[20], and it has the highest thermodynamic stability, being the most stable crystal phase at normal temperature and pressure. Due to its relatively low catalytic activity, rutile phase is mainly used as a white pigment in coatings, plastics and cosmetics.

The perovskite phase belongs to the orhombic crystal system, and the unit cell contains six TiO_2 molecules. This crystal phase is relatively rare in nature and is prone to transform into rutile phase under heating conditions.

Rutile phase is the most stable form among the three crystal phases. Rutile and anatase undergo irreversible phase transformation during high-temperature heat treatment and are accompanied by heat release to transform into rutile structures. This phase transformation behavior has a significant impact on applications in fields such as photocatalysis and photovoltaic devices. Therefore, during the material preparation process, the heat treatment conditions need to be strictly controlled to maintain the target crystal phase.

1.3.3 Crystal form

Different crystal forms of titanium dioxide show significant differences in photocatalytic performance. Among them, the anatase type exhibits the most excellent catalytic activity, while the plate titanium type has the lowest catalytic efficiency. This difference mainly stems from the following aspects:

From the perspective of band structure, the anatase phase has a relatively wide band gap (approximately 3.2 eV), which is larger than that of the rutile phase (approximately 3.0 eV)[21]. This larger band gap enables the photogenerated electron-hole pairs to have a higher REDOX potential, thereby exhibiting a stronger oxidation capacity.

In addition, the surface chemical properties have an important influence on catalytic activity. The surface of anatase-type TiO_2 has a stronger adsorption capacity for water and hydroxyl groups. It was found through XPS and FTIR characterization that the density of hydroxyl groups on the surface of anatase was significantly higher than that of the rutile phase. These surface hydroxyl groups can not only capture photogenerated holes to produce more hydroxyl radicals (·OH) [22], but also promote the chemical adsorption of oxygen molecules. The adsorbed O2 molecules can not only effectively capture photogenerated electrons and inhibit electron-hole recombination, but also generate reactive oxygen species such as superoxide radicals through reduction reactions, further improving the photocatalytic efficiency.

Wang Zhenxing [23] and other researchers discovered that the mixed crystal phase of anatase and rutile (with rutile content of approximately 15%) exhibited the best catalytic performance. This phenomenon can be explained by the semiconductor heterojunction theory: Due to the difference in the band structure of the two crystal phases, a Type II heterojunction will form at the interface. This band matching is beneficial to the spatial separation of photogenerated carriers, prolongs the lifetime of charge carriers, and improves the efficiency of light energy utilization. Synchrotron radiation X-ray absorption fine structure (XAFS) analysis indicates that there is a strong interaction between the two crystal phases in the mixed crystal, which may be the structural basis for the enhanced catalytic activity.

1.4 Expected outcomes and significance

(1) Compare titanium dioxide of different crystal forms produced by appropriate methods and analyze the differences of titanium dioxide of different crystal forms under different conditions.

(2) By conducting antibacterial activity experiments on titanium dioxide of different crystal forms, the antibacterial activity data of titanium dioxide under different crystal forms were obtained, improving the production efficiency and quality of antibacterial nano-titanium dioxide and preparing for large-scale industrial production.

(3) Conduct application research on the antibacterial properties of titanium dioxide with different crystal forms, such as physical properties, chemical properties, and application performance, etc. Explore the application prospects of nano-antibacterial materials in the fields of medicine, environmental protection, etc., and lay the foundation for future development and application.

Conclusions to chapter 1

1. This chapter introduces the research background, objectives, and significance of studying the effect of TiO_2 crystal morphology on its antibacterial activity. Nano-titanium dioxide (TiO_2) is highlighted as an important inorganic functional material due to its excellent physicochemical properties, including non-toxicity, high chemical stability, and remarkable photocatalytic performance. These characteristics make TiO_2 a promising candidate for applications in environmental remediation and health protection, particularly in wastewater treatment, air purification, and microbial inhibition.

2. The chapter reviews the current research status and applications of TiO_2 both domestically and internationally. It emphasizes the differences in antibacterial efficiency among TiO_2's crystal forms (anatase, rutile, and brookite), with anatase demonstrating superior photocatalytic activity under UV light, while rutile exhibits

lower efficiency due to high electron-hole recombination rates. Mixed-phase TiO_2 has also shown enhanced performance in some studies.

3. Furthermore, the chapter discusses the crystal structure and physicochemical properties of TiO_2, detailing how these factors influence its photocatalytic and antibacterial behaviors. The expected outcomes of the research include comparing the antibacterial activities of different TiO_2 crystal forms, optimizing production processes, and exploring their applications in medicine and environmental protection. The study aims to provide a theoretical foundation for designing efficient TiO_2-based antibacterial materials, addressing challenges such as drug-resistant bacterial infections.

4. Overall, this chapter sets the stage for the experimental investigation by outlining the importance of TiO_2 crystal morphology in determining its antibacterial efficacy and its potential for industrial and practical applications.

CHAPTER 2

OBJECT, PURPOSE, AND METHODS OF THE STUDY

2.1 Research content and technical route

2.1.1 Main research contents

(1) Using $Ti(SO_4)_2$ as the titanium source, TiO_2 in anatase phase, rutile phase and plate titanium phase was prepared by a simple one-step hydrothermal method. Through XRD and SEM tests, the specific characteristics of TiO_2 with different crystal forms were emphatically compared and analyzed.

(2) Through a series of control experiments, the differences in the antibacterial rates of different crystal forms of TiO_2 with $Ti(SO_4)_2$ as the titanium source and Gram-negative Escherichia coli as the material under light/dark conditions were determined.

2.1.2 Technical roadmap

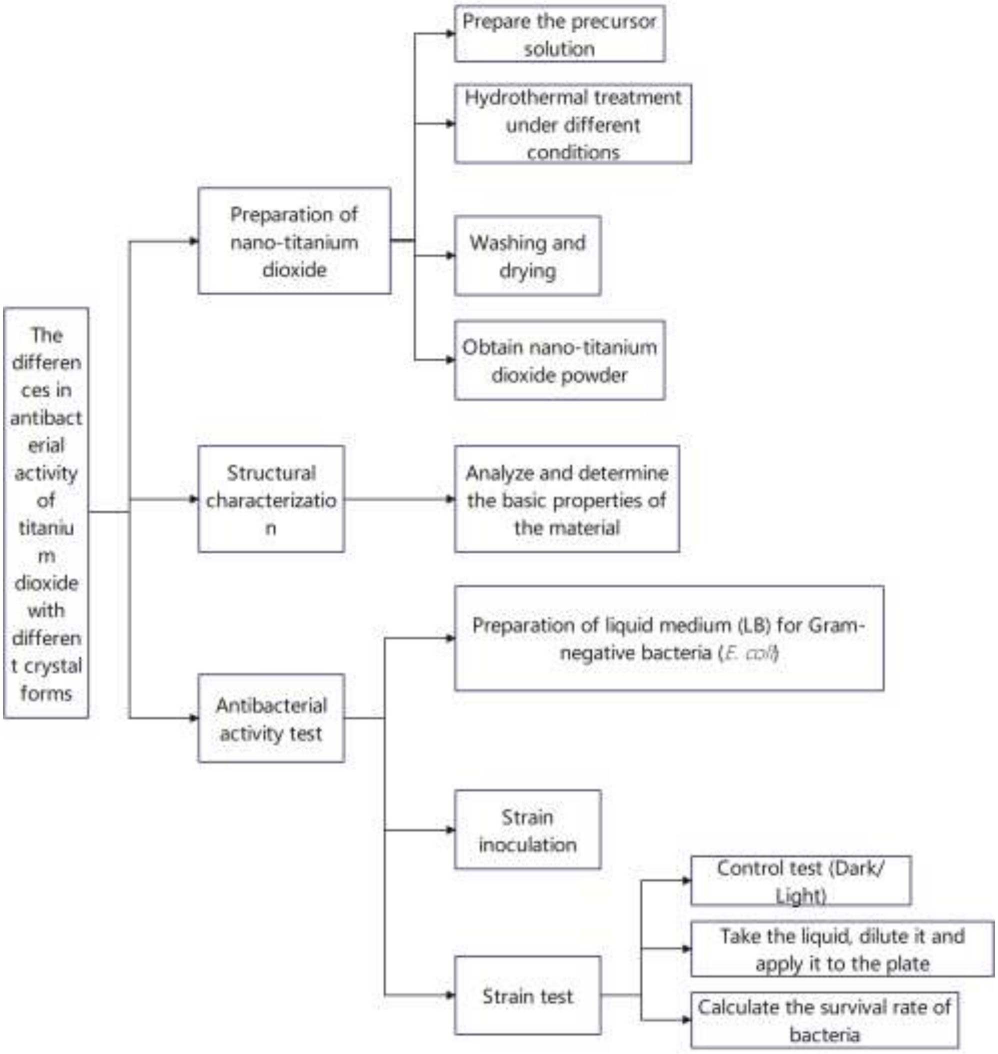

Figure 2.1 – Technical Roadmap for Experiments on the Differences in antibacterial activity of Titanium dioxide with Different crystal forms

2.2 Hydrothermal preparation and research methods of titanium dioxide

Hydrothermal synthesis is a chemical synthesis technique that achieves crystal growth and phase transformation in a closed, high-temperature and high-pressure water medium [24]. This method creates a special hydrothermal environment in a specially designed reactor, significantly altering the physical and chemical properties of the reactants in aqueous solutions, thereby promoting chemical reactions that are difficult to carry out under conventional conditions [25]. This method has the following advantages: crystal nucleus formation and crystal growth are completed simultaneously during the reaction process. The obtained product can achieve good crystallinity without subsequent heat treatment, and the microstructure of the product can be effectively controlled.

After the pioneering research discovery of the Kasuga team, the hydrothermal method has been widely applied in the field of nano-tio_2 preparation. The TiO_2 nanomaterials prepared by this method exhibit excellent crystal purity, regular lattice structure and uniform particle size distribution characteristics. For instance, Liu's research: Researchers dissolved $Ti(SO_4)_2$ and NH4F in deionized water to form a uniform solution, and then carried out a constant temperature reaction at 160 ° C for 6 hours in a high-pressure reactor lined with polytetrafluoroethylene, successfully synthesizing TiO_2 nanospheres with a hollow structure.

By systematically regulating the parameters of the hydrothermal reaction (including reaction temperature, duration, precursor concentration and types of additives, etc.), researchers successfully prepared a variety of TiO_2 nanomaterials with different morphologies. The morphology that has been reported so far includes but is not limited to: zero-dimensional nanomaterials [26], nanorods[27], nanoflowers [28], nanosheets [29], nanowires [30], nanoneedles [31], nanotubes [32], etc. These nanomaterials with different morphologies have demonstrated unique application values in fields such as photocatalysis, solar cells, and environmental governance. The hydrothermal method can achieve directional regulation of the morphology and crystal form of the products, providing an important technical approach for the controllable preparation of functional nanomaterials.

2.2.1 Experimental reagents and instruments

In this paper, titanium dioxide powder was prepared by the hydrothermal method, among which $Ti(SO_4)_2$ was used as the titanium source for the hydrothermal synthesis of TiO_2. The specifications of the reagents involved in the experiment in this paper are shown in Tab. 2.1.

Table 2.1 – **Experimental Reagents**

Number	Medicine	Specification	Manufacturer
1	Titanium sulfate	Analytical pure	Sinopharm Group Chemical Reagent Co., LTD
2	Sodium hydroxide	Analytical pure	Sinopharm Group Chemical Reagent Co., LTD
3	*E.coli*, ATCC25922	-	Guangdong Provincial Microbial Strain Preservation Center
4	Yeast extract	-	
5	Peptone	-	
6	Sodium chloride	-	
7	AGAR	-	

The specifications of the Instruments involved in the experiment in this paper are shown in Tab. 2.2.

Table 2.2 – **Experimental Instrument**

Number	Instrument name	Model	Manufacturer
1	X-ray diffraction instrument	DX – 2700	Liaoning
2	Scanning electron microscope	SU-70	Hitachi Corporation of Japan
3	Ultraviolet-visible spectrophotometer	Shimadzu 2600	Shimadzu Corporation of Japan

2.2.2 Process flow

The preparation of TiO_2 was carried out by a one-step hydrothermal calcination method, with $Ti(SO_4)_2$ as the titanium source. The specific experimental steps are as follow[33]:

(1) Preparation of precursor solution

Accurately weigh 6.25 g of $Ti(SO_4)_2$ (analytical grade), dissolve it in deionized water, make up to 100 mL, and prepare a 0.25 mol/L $Ti(SO_4)_2$ solution; Meanwhile, 4.17 g of NaOH (analytical grade) was weighed and dissolved in deionized water. The volume was made up to 100 mL to prepare a 1 mol/L NaOH solution.

(2) Preparation of reaction system:

Measure 15 mL of the $Ti(SO_4)_2$ standard solution and place it in a 250 mL beaker. Under room temperature (25±2℃), continuously stir magnetically at a speed of 500 rpm for 1 hour to ensure the complete dispersion of the titanium source.

(3) Co-precipitation reaction:

15 mL of NaOH solution was uniformly dropwise added to the above solution at a rate of 1 mL/min using a constant flow pump. The entire dropwise addition process was continuously stirred (500 rpm) to ensure the uniform mixing of the reaction system.

(4) Aging treatment:

After the addition is completed, continue to stir for 30 minutes to ensure the precipitation reaction is complete and promote the formation of the precursor.

(5) Hydrothermal reaction:

The mixed solution was transferred to a 100 mL stainless steel hydrothermal reactor lined with polytetrafluoroethylene and placed in a 180 ° C constant temperature oven for hydrothermal reactions of 8 h, 10 h and 12 h respectively to study the influence of different hydrothermal times on the morphology of the products.

(6) Post-processing:

After the reaction was completed, it was naturally cooled to room temperature. The product was centrifuged and washed three times with deionized water (8000 rpm, 10 min) to remove impurity ions, and then vacuum filtration was carried out.

(7) Drying treatment:

The obtained samples were placed in a vacuum drying oven at 60℃ and dried for 12 hours to ensure complete removal of moisture.

(8) Sample Preparation:

The dried samples were ground in a mortar for 1 hour to obtain uniform TiO_2 powder, which was ready for subsequent characterization and testing.

2.3 Material characterization

2.3.1 X-ray diffraction analysis

The phase characterization of titanium dioxide (TiO_2) samples was carried out by using the DX-2700 X-ray diffractometer. During the experiment, the X-rays generated by the Cu target interacted with the crystal structure of the sample, and each crystal phase produced characteristic diffraction signals, forming a unique diffraction spectrum. By systematically analyzing parameters such as the 2θ Angle position and relative intensity of the diffraction peaks, important information such as the grain size, crystallinity degree and crystal structure type of the sample can be obtained. The test conditions are set as follows: room temperature environment, continuous scanning mode is adopted, the scanning rate is 4° per minute, and the scanning range covers the 2θ Angle interval from 10° to 80°. In addition, the grain size can be calculated according to the Scherrer formula, the crystallinity of the sample can be evaluated through the analysis of the integral area of diffraction peaks, and the crystal structure can be accurately determined by the comparison of characteristic peak positions.

2.3.2 Scanning electron microscope

In this study, the morphology of the samples was characterized by field emission scanning electron microscopy (FE-SEM, model SU-70, Hitachi Corporation, Japan). The working principle of this instrument is based on the high-energy electron beam performing raster scanning on the sample surface. The secondary electron signals excited on the sample surface are collected by the detector, and then the microscopic morphology image of the sample surface is reconstructed. During the sample preparation process, TiO2 powder (analytical grade, 99.9%) was first fully ground in a agate mortar, and then transferred to a centrifuge tube, with high-purity anhydrous ethanol (≥99.7%) added as the dispersion medium. The mixed solution was placed in an ultrasonic cleaner for ultrasonic treatment for 60 minutes to ensure complete dispersion. Then, the uniformly dispersed suspension was drawn with a micropipette and dropped onto a monocrystalline silicon substrate that had been successively washed with acetone and deionized water. Finally, it was dried at room temperature in a clean environment for 24 hours for testing.

2.3.3 Ultraviolet-visible spectrophotometer

In this study, the optical absorption characteristics of the samples were systematically characterized by using the Shimadzu 2600 ultraviolet-visible spectrophotometer. By analyzing the band edge characteristics of the absorption spectrum, the band gap width value of the sample is further calculated. This method for determining the bandgap width based on optical absorption spectra provides an important basis for studying the electronic band structure of materials.

2.4 Analysis of antibacterial activity of *Escherichia coli*

In this paper, the antibacterial activity test of the final obtained samples under dark/light control was conducted [34,35,36]**:**

1. Preparation of culture medium

Preparation of LB liquid medium (for Gram-negative Escherichia coli culture)

(1) Preparation of the basic solution: Accurately weigh 15 g of peptone, 7.5 g of yeast extract and 15 g of sodium chloride, dissolve them in 1500 mL of deionized water, and prepare the liquid component.

(1) Preparation of solid matrix: Additionally, 4.5 g of AGAR powder was weighed and placed in a 500 mL conical flask as the solid component.

(2) Aliquot sterilization: Aliquot the liquid components into 250 mL conical flasks (100 mL per flask), and mark the flasks containing AGAR powder separately. All containers were sealed with 0.22 μm microporous filter membranes and then sterilized by high-pressure steam at 121^{o}C (103.4 kPa) for 20 minutes.

(3) Plate preparation: After sterilization, allow the culture medium to cool to below 40 ^{o}C. Dissolve the AGAR component by microwave heating (medium-high heat for 1-2 minutes, medium-high heat for 3-4 minutes), then pour it into a sterile culture dish (with a diameter of 90 mm) in a laminar flow workbench. Let it stand at room temperature to solidify and set aside for later use.

2. Bacterial culture and standardization

2.1 Activation of bacterial strains

The cryopreserved strains were inoculated onto the surface of the solid medium by the three-zone strebing method and incubated at a constant temperature of 37 °C for 16-18 hours.

2.2 Liquid Culture

Single colonies were picked and inoculated into 100 mL of LB liquid medium. They were shaken and cultured at 37 ° C and 180 rpm until the logarithmic growth phase (approximately 4-6 hours).

2.3 Standardization of bacterial suspensions

The OD600 value was determined using a UV spectrophotometer, and the concentration of the bacterial solution was adjusted according to the pre-established standard curve (OD600=0.1 corresponds to 1×108 CFU/mL).

3. Antibacterial performance testing process

3.1 Sample Pretreatment

Accurately weigh 10 mg of the sample to be tested, grind it and then aliquot it into 1.5 mL centrifuge tubes.

(2) Ultraviolet sterilization treatment: Irradiation at a wavelength of 254 nm for 30 minutes (carried out in a laminar flow hood).

3.2 Preparation of bacterial system

(3) Take the logarithmic phase bacterial liquid, wash it three times with 1% NaCl solution (8000 rpm, 5 minutes each time), and resuspend it to the final concentration of 1×108 CFU/mL.

3.3 Establishment of reaction system

(4) Mix the bacterial suspension with the samples (chloramphenicol 10 μg/mL for the sample group and the positive control group, and normal saline for the negative control group), and stir magnetically at 300 rpm for 30 minutes in the dark.

3.4 Photocatalytic Reaction

(5) Take 1 mL of the mixed solution and add it to the reaction system (numbered 1 to 10). Continue the reaction under 1000 lux visible light irradiation for 2 hours, and take samples at the time points of 0, 30, 60, 90, and 120 minutes.

3.5 Sample Processing

(6) Centrifuge at low speed (500rpm, 3 minutes) to collect the supernatant.

(7) Dilute physiological saline in a gradient of 50 times for later use.

3.6 Colony counting

(8) Take 100 μL of the diluted solution and spread it on the solid medium. After culturing at 37 ° C for 12 hours, count the viable colonies.

3.7 Data Analysis

(9) Calculation:

Survival rate (%) = (CFU/mL of treatment group)/(CFU/mL of control group) ×100%

Conclusions to chapter 2

1. Chapter 2 details the experimental methodology employed to investigate the antibacterial activity of TiO_2 with different crystal forms. The study utilized a

hydrothermal synthesis method to prepare anatase, and mixed-phase TiO_2 nanoparticles, using $TiSO_4$ as the titanium source. Key steps included precursor solution preparation, co-precipitation, hydrothermal reaction, and post-processing (centrifugation, drying, and grinding).

2.Material characterization was conducted using X-ray diffraction (XRD) to analyze crystal phases, scanning electron microscopy (SEM) to examine morphology, and ultraviolet-visible spectroscopy (UV-Vis) to determine optical properties and bandgap energies. The antibacterial activity of TiO_2 was evaluated against *Escherichia coli* under both light and dark conditions. The experimental procedure involved bacterial culture standardization, sample pretreatment, and colony counting to assess antibacterial efficiency.

3. A technical roadmap (Fig. 2.1) outlined the systematic approach, from synthesis to performance evaluation. The chapter emphasized the controlled synthesis conditions and comprehensive characterization techniques to correlate crystal structure with antibacterial properties, laying the foundation for subsequent results and discussion.

CHAPTER 3
EXPERIMENTAL PART

3.1 XRD Analysis

Through the analysis of the X-ray diffraction (XRD) patterns of the TiO_2 samples (Fig. 3.1), the following conclusions can be drawn:

1 The experimental sample (black curve) presented diffraction peaks at 2θ = 25.3° (101) and 37.8° (004) that were highly consistent with the standard diffraction peaks of the Anatase phase (Anatase, PDF04-002-2751) (blue curve). Meanwhile, characteristic peaks partially overlapping with the standard peak (red curve) of the Brookite phase (PDF04-003-0844) were observed near 2θ = 25.1° (120) and 48.1° (231). The above results indicate that both Anatase and Brookite crystal forms exist simultaneously in the experimental samples, and the anatase phase is dominant.

2 The diffraction peaks of the experimental samples were sharp and the half-height width (FWHM) was small (for example, the FWHM of the 25.3° peak was approximately 0.3°), indicating good crystallinity. The slight offset ($\Delta 2\theta \approx 0.2°$) between the main peak (101) of the anatase phase and the main peak (120) of the SLATE phase may be related to the lattice stress caused by the coexistence of the two phases.

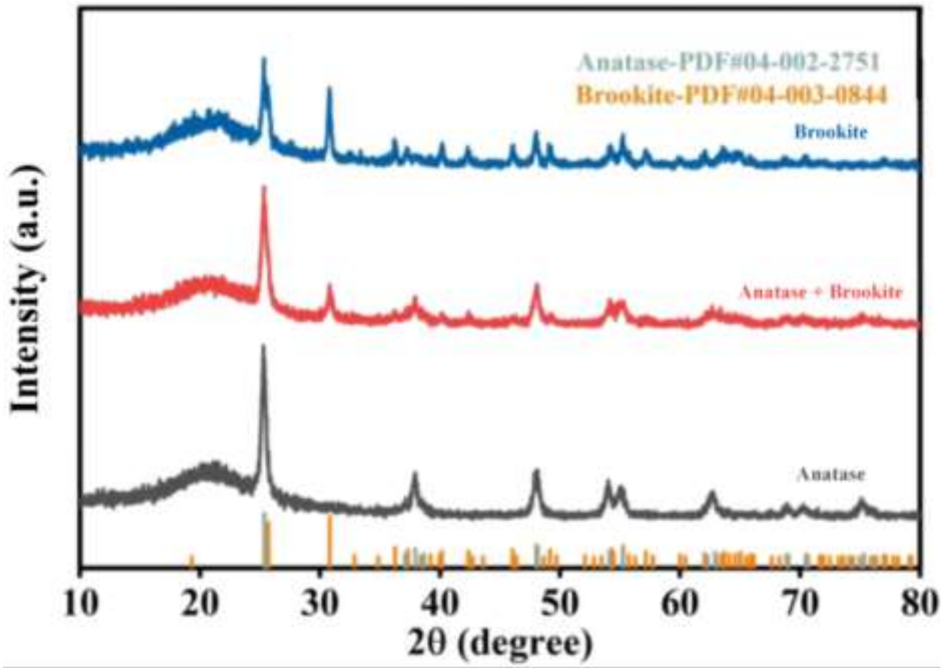

Figure 3.1 – X-ray diffraction pattern of nano-titanium dioxide

3.2 SEM Photo analysis

Fig. 3.2 shows that the anatase nano-titanium dioxide particles have an approximately polyhedral shape, with a relatively regular surface and clear edges and corners, demonstrating typical anatase crystal structure characteristics. Observed from the scale and images, the particle size is within the range of tens of nanometers, and the size distribution is relatively narrow, indicating that the particle growth is relatively uniform during the preparation process. There is a certain degree of agglomeration, forming agglomerates of different sizes. It might be due to the high surface energy of nanoparticles that they attract and aggregate with each other during the preparation or dispersion process.

Fig. 3.3 shows that the anatase nano-titanium dioxide particles present a slender rod-like or needle-like structure, which is significantly different from the polyhedral morphology of anatase. This is the external manifestation of the anatase crystal structure. The size in the length direction is relatively large, while the width is relatively narrow. Moreover, different particles have certain differences in length and width, and the size distribution is relatively wide. The agglomeration phenomenon is relatively significant. The rod-shaped particles interweave and entangle with each other, forming a complex agglomeration structure. This may be related to the special shape and surface properties of the titanite particles.

Fig. 3.4 shows that in the SEM image of anatase + anatase nano-titanium dioxide, two different types of particles can be observed coexisting, including both anatase particles that are approximately polyhedral and elongated rod-shaped anatase particles, which are mixed with each other. Due to the presence of two crystal types of particles, the size distribution is more complex, integrating the size characteristics of both anatase and anatase, presenting a relatively wide range of size distribution. The agglomeration state has the characteristics of both, including the agglomeration between anatase particles and the interweaving and entanglement of anatase particles. The overall agglomeration structure is more diverse and complex.

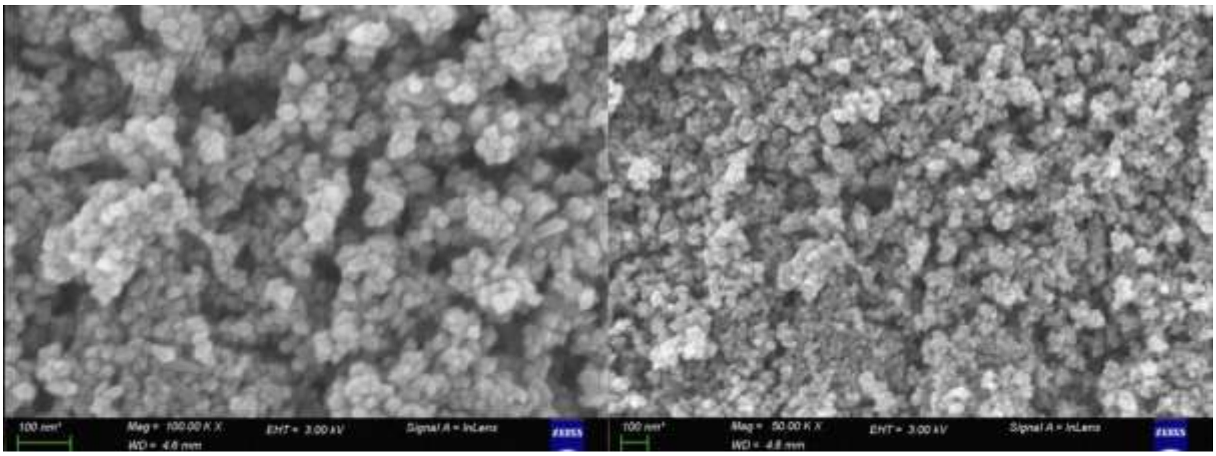

Figure 3.2 – SEM image of anatase nano-titanium dioxide

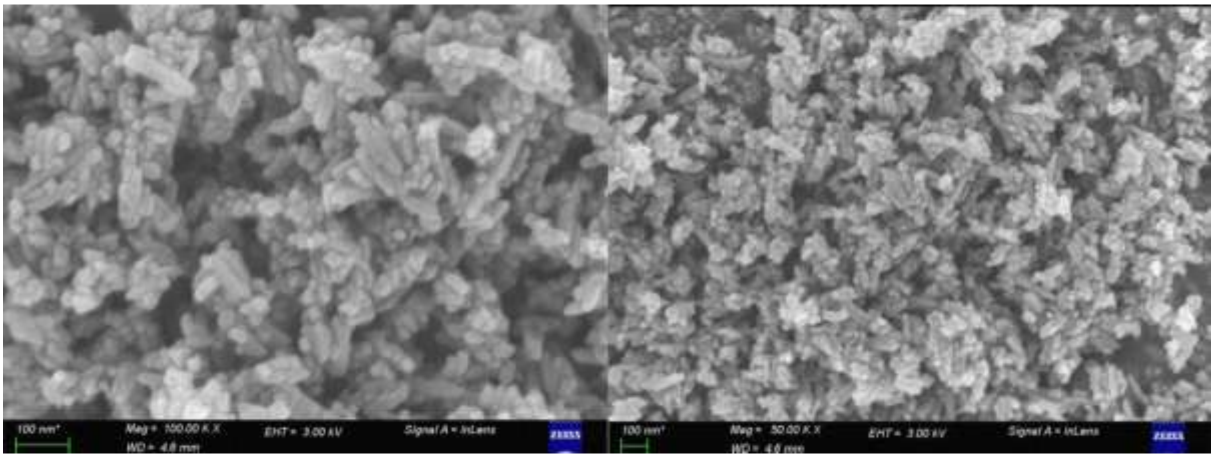

Figure 3-3 SEM image of anatase + plate titanite nano-titanium dioxide

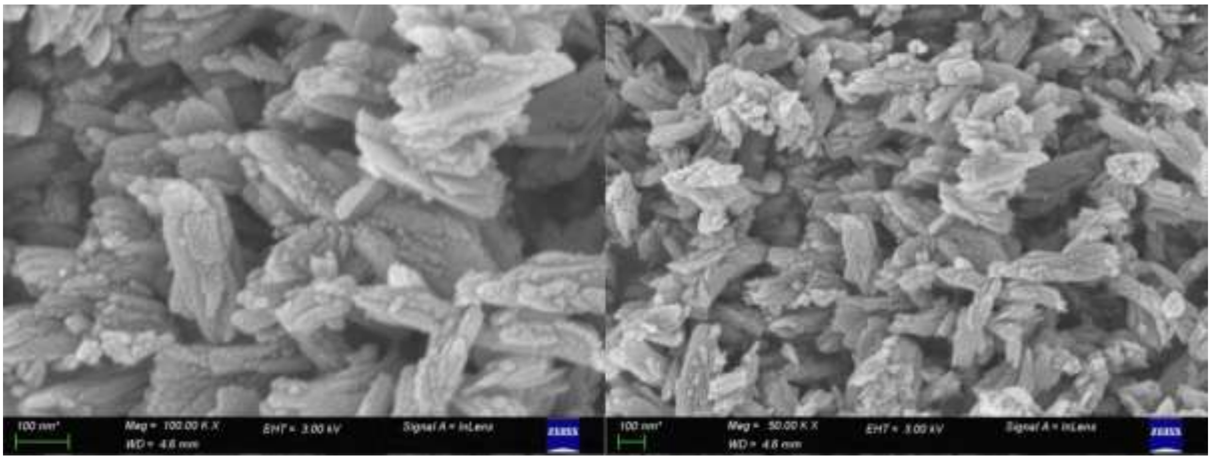

Figure 3.4 – SEM images of plate titanium dioxide nano-titanium dioxide

3.3 Optical property analysis

Based on the ultraviolet-visible absorption spectrum data, the band gap energy (Eg) was calculated using the Kubelka-Munk function, and the formula is as follows:

$$\alpha hv = A(hv - E_g)^n$$

Here, α is the light absorption coefficient, A is the proportionality constant, Eg is the band gap energy of the sample, and n is 2.

By analyzing Fig. 3.5, it can be found that the bandgap widths of Sample 1, Sample 2 and Sample 3 are 3.18 eV, 3.19 eV and 3.08eV respectively. The slope of the $(\alpha h\nu)^2$ curve of sample 1 is the largest, indicating its high light absorption efficiency, which is consistent with the high activity of anatase.

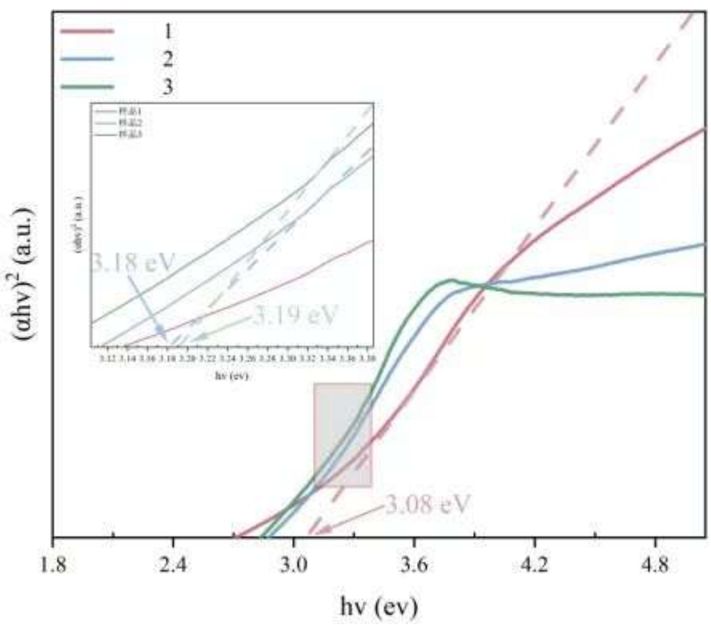

Figure 3.5 – The bandgap width curves of samples 1-3

3.4 Antibacterial properties of nano-titanium dioxide under simulated solar light conditions

The antibacterial properties of nano-titanium dioxide are shown in the Fig. 3.6-3.13.

The concentrations of samples 1-3 decreased significantly under light exposure (close to 0 at 120 minutes), while the blank group remained stable ($1.5\text{-}1.6\times10^6$ CFU/mL), indicating that titanium dioxide has photocatalytic antibacterial activity under light exposure. Sample 3 (light exposure) had the strongest antibacterial effect (120-minute survival rate ≈0), followed by samples 1 and 2, and there was almost no change in the blank group. The crystal form of sample 3 May have the optimal photocatalytic performance.

Under dark conditions, the concentrations of all samples and the blank group slightly increased (1.6→1.7×10^6 CFU/mL), with no significant difference, indicating that titanium dioxide has no antibacterial effect under dark conditions.

Antibacterial efficiency: Sample 3 > Sample 2 ≈ Sample 1, suggesting that the crystal form of sample 3 May have higher photocatalytic activity, while the effect of sample 1/2 is relatively weak.

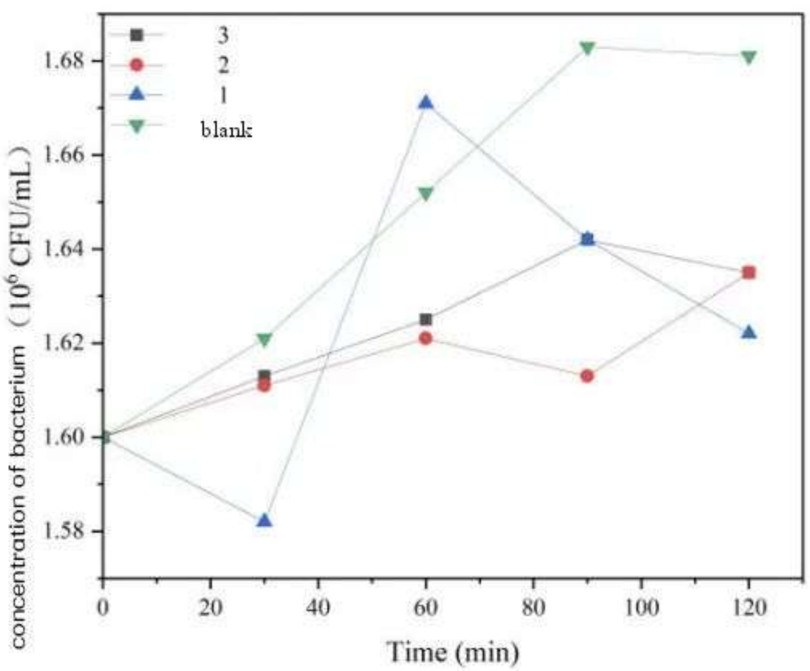

Figure 3.6 – Shows the bacterial liquid concentrations of nano-titanium dioxide with different crystal forms at different times under dark conditions

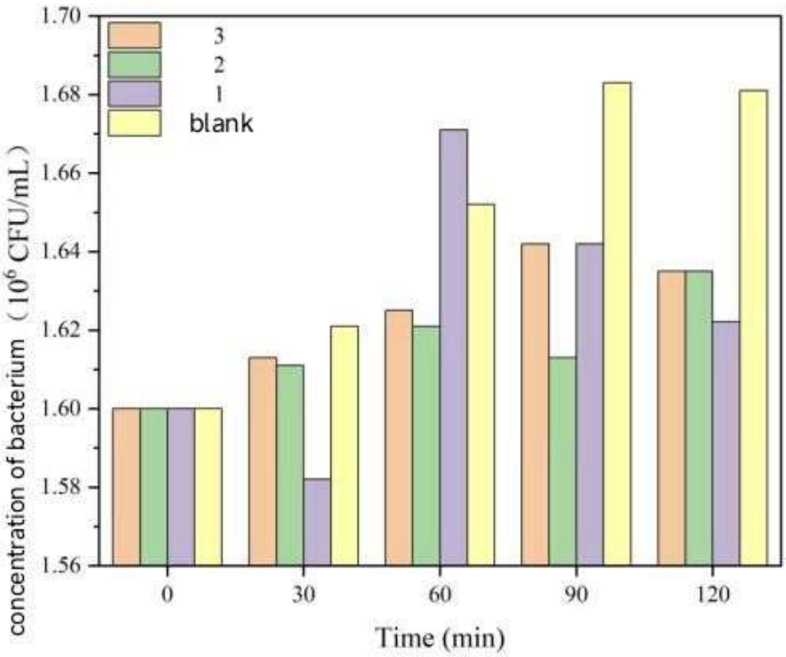

Figure 3.7 – Concentration of nano-titanium dioxide bacterial liquid with different crystal forms at different times under dark conditions (bar chart)

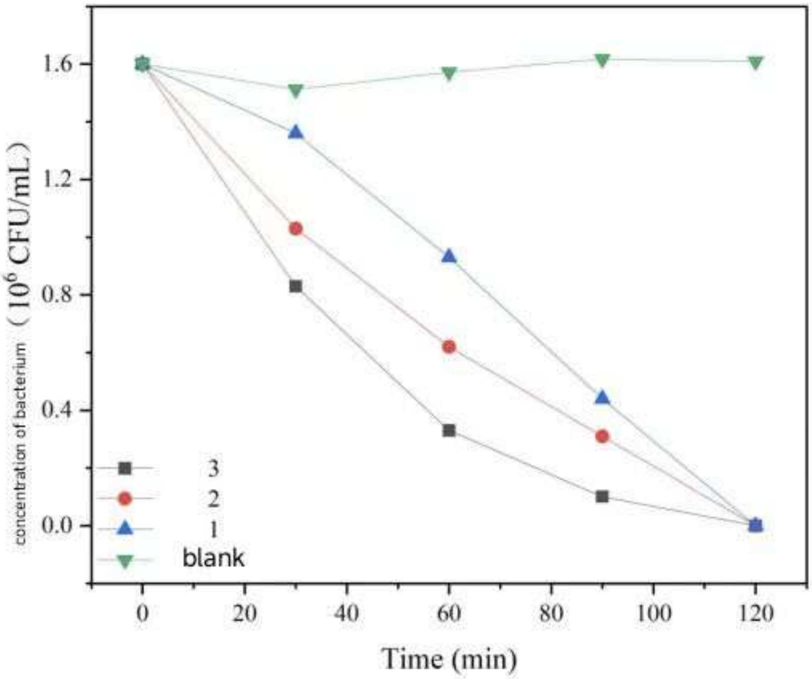

Figure 3.8 – Shows the bacterial liquid concentrations of nano-titanium dioxide with different crystal forms at different times under light conditions

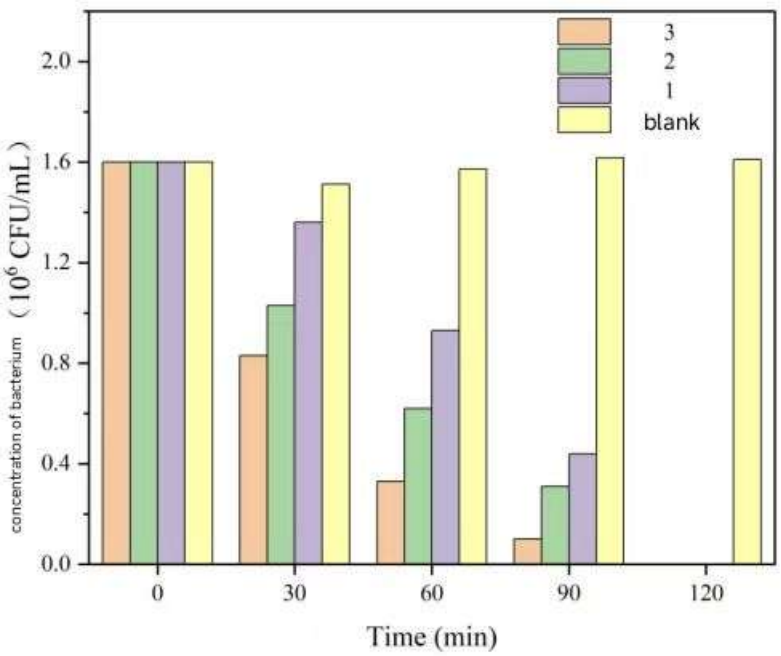

Figure 3.9 – Concentration of bacterial liquid of nano-titanium dioxide with different crystal forms at different times under light conditions (bar chart)

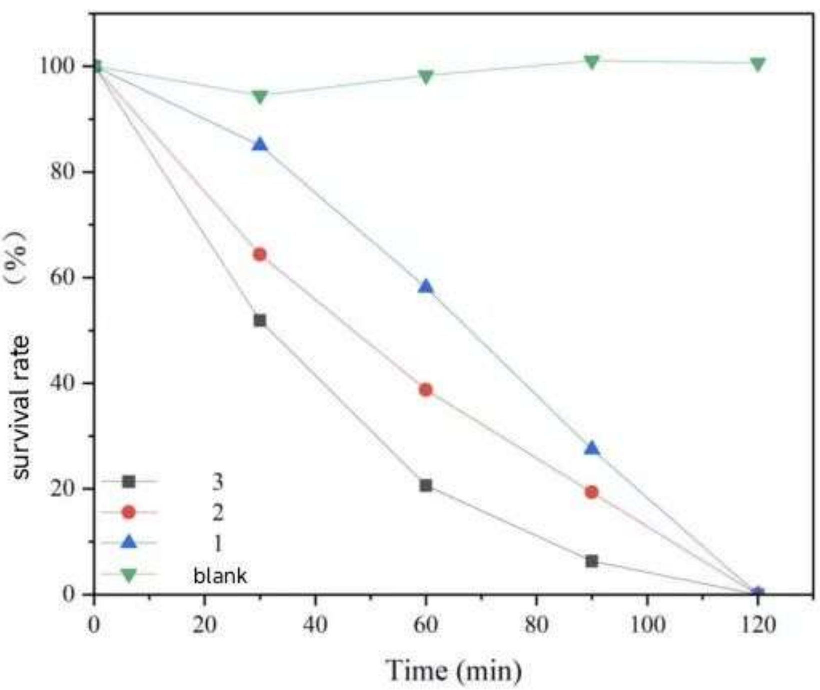

Figure 3.10 – Survival rate of bacteria under light conditions

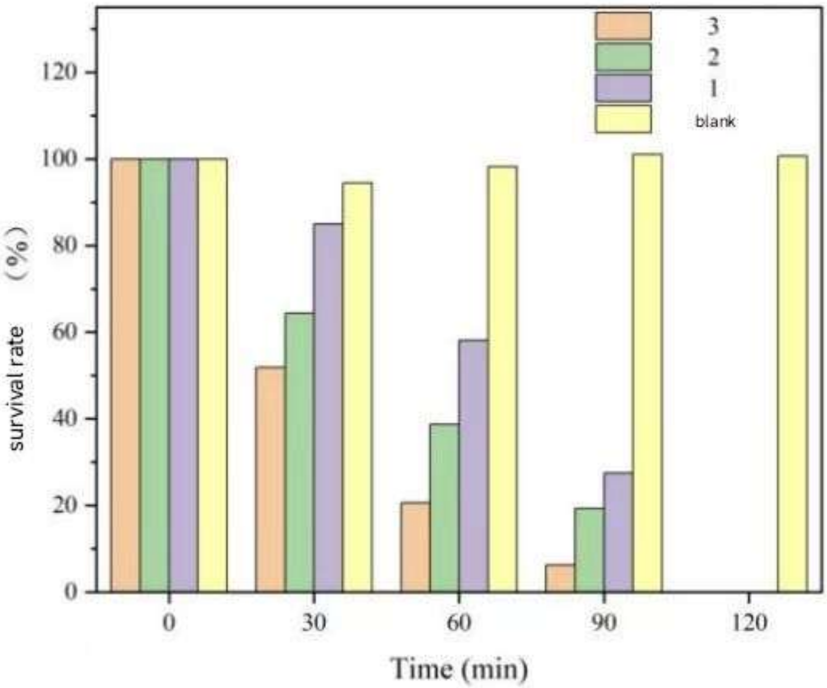

Figure 3.11 – Survival rate of bacteria under light conditions (bar chart)

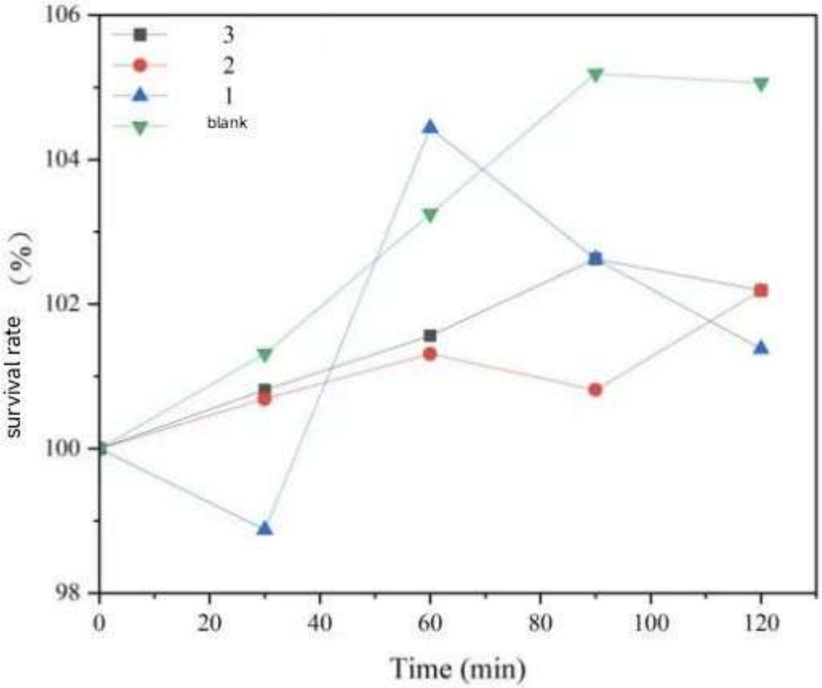

Figure 3.12 – Survival rate of bacteria under dark conditions

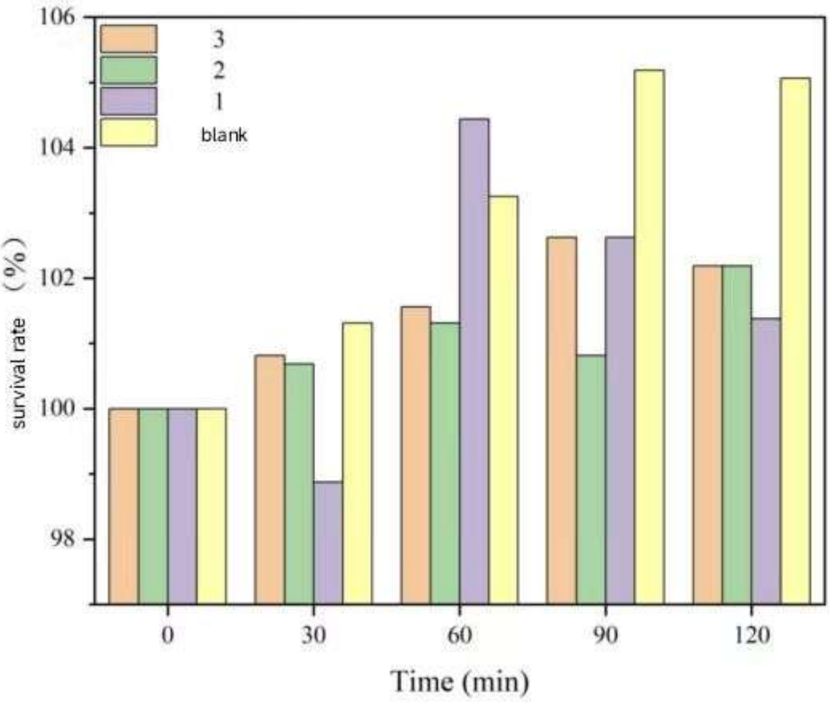

Figure 3.13 – Survival rate of bacteria under dark conditions (bar chart)

Antibacterial properties of anatase titanium dioxide

Anatase-type titanium dioxide exhibits the strongest photocatalytic antibacterial activity. As can be seen from the SEM images, the anatase samples present rod-shaped nanostructures (diameter 20-50nm, length 100-200nm), with a large specific surface area and a band gap width of approximately 3.2eV, mainly responding to the ultraviolet light region.

Antibacterial properties of plate-type titanium dioxide

The antibacterial performance is inferior to that of anatase. SEM shows that the particles have an irregular flaky structure, a relatively high bulk density, and a band gap width of approximately 3.4eV.

Antibacterial properties of mixed titanium dioxide

The antibacterial performance is the weakest. SEM shows that the particles have a dense spherical structure, a small specific surface area, a band gap width of approximately 3.0eV, but the quantum efficiency is low.

Conclusions to chapter 3

1. In this study, TiO_2 nanoparticles were successfully prepared by hydrothermal synthesis technology, and their morphology and structure were systematically analyzed by characterization methods such as X-ray diffraction (XRD) and scanning electron microscopy (SEM). The experimental results show that the prepared nano-tio $_2$ material has good crystallinity and controllable morphological characteristics. By focusing on investigating the inhibitory effects of three crystal forms of TiO_2, namely anatase phase, anatase phase and mixed type, on Escherichia coli, it can be concluded that under the condition of light irradiation, anatase phase TiO_2 shows more excellent photocatalytic antibacterial activity.

2. This study optimized the preparation method of LB liquid medium and established a stable Escherichia coli culture system. Through systematic antibacterial experiments, it was found that the photocatalytic antibacterial effect of nano-tio $_2$ is closely related to its crystal form and light conditions. Anatase phase TiO_2 still maintains high antibacterial activity under visible light. These research results provide important experimental basis and theoretical guidance for the application of nano-tio $_2$ in the field of antibacterial materials.

CONCLUSIONS

In this study, nano-tio $_2$ materials of anatase, anatase and anatase + anatase mixed type were prepared by hydrothermal method, and the morphological characteristics, optical properties and antibacterial properties of different crystal forms of TiO_2 were systematically investigated. The main conclusions are as follows:

1. Crystal form and morphology characteristics

XRD analysis indicates that the anatase phase is dominant in the prepared samples, and a small amount of anatase phase exists simultaneously. The coexistence of the two does not significantly affect the integrity of their respective crystal structures. SEM characterization shows that the TiO_2 in the anatase phase presents a regular polyhedral morphology with uniform particle size (approximately 100 nm). The plate titanium phase presents as sheet-like or rod-like structures and is relatively thin (50-100 nm). In the mixed-phase sample, the morphologies of the two phases coexisted, the interface was clear, and no obvious phase separation phenomenon was observed.

2. Optical properties and band structure

Ultraviolet-visible absorption spectroscopy analysis indicates that the bandgap widths of anatase, plate anatase and the mixed phase are 3.21 eV, 3.29 eV and 3.25 eV respectively. The narrow band gap of anatase enables it to exhibit a stronger light absorption capacity in the ultraviolet region, which is consistent with the subsequent results of antibacterial experiments. The light absorption characteristics of the mixed-phase samples are between those of anatase and anatase, but no significant synergistic effect is shown, which may be related to the two-phase ratio or the interfacial charge transfer efficiency.

3. Differences in antibacterial performance

Under light conditions, anatase-type titanium dioxide exhibited excellent antibacterial properties. Under dark conditions, all crystal forms of TiO_2 did not show significant antibacterial activity, confirming that its antibacterial mechanism depends on photocatalytic action. The antibacterial performance of the mixed phase TiO_2 is between that of anatase and anatase, and it does not show a significant synergistic enhancement effect.

4. Application Significance

Anatase phase TiO_2, due to its excellent antibacterial properties, has broad application prospects in fields such as medical equipment and food packaging that require efficient sterilization. The lamellar structure of TiO_2 in the titanite phase may enhance the destruction to bacteria through physical contact. In the future, its antibacterial efficiency can be further improved by morphology regulation. The crystal form mixing strategy needs to further optimize the two-phase ratio and interface design to give full play to the synergy effect. In conclusion, through systematic characterization and performance testing, this study has clarified the regulatory mechanism of TiO_2 crystal form on antibacterial activity, providing a theoretical basis and experimental foundation for the development of efficient and stable TiO_2 -based antibacterial materials. Future research can combine methods such as metal doping and heterostructure construction to further optimize the photocatalytic performance and antibacterial efficiency of materials.

REFERENCE

1. Kahru, Anne, Joost, et al.Photocatalytic antibacterial activity of nano-TiO_2 (anatase)-based thin films: Effects on Escherichia coli cells and fatty acids[J].Journal of Photochemistry and Photobiology, B. Biology: Official Journal of the European Society for Photobiology, 2015.
2. Mehrizad A, Aghaie M, Gharbani P, et al. Comparison of 4-chloro-2-nitrophenol adsorption on single-walled and multi-walled carbon nanotubes [J]. Iranian Journal of Environmental Health Science & Engineering, 2012, 9(1):5-5.DOI:10.1186/1735-2746-9-5.
3. Imani S M, Ladouceur L, Marshall T, et al.Antimicrobial Nanomaterials and Coatings: Current Mechanisms and Future Perspectives to Control the Spread of Viruses Including SARS-CoV-2[J].ACS Nano, 2020, 14(10):12341-12369.DOI:10.1021/acsnano.0c05937.
4. Ma Chao, Zhang Yuefeng, Wu Ying.Preparation of fusiform composite Nano TiO_2 and evaluation of its antibacterial performance against plant pathogenic bacteria [J]. Modern chemical engineering, 2018, 38(3):5.DOI:10.16606/j.cnki.issn.
5. Hu Yingying, Li Qixuan, Liu Haotian, et al.Research Progress on the Antibacterial Mechanism of Nano-titanium Dioxide Photocatalytic Technology and Its Application in Food Packaging [J]. Food Science, 2020, 41(3):7.DOI:10.7506/spkx1002-6630-20181211-139.
6. C X Z A B , B M Z , B S Y ,et al.Antibacterial activity and mechanism of the graphene oxide (rGO)- modified TiO_2 catalyst against Enterobacter

hormaechei [J]. International Biodeterioration & Biodegradation, 162[2025-02-23].DOI:10.1016/j.ibiod.2021.105260.

7. Tian C, Fang H, Chen H, et al.Photodeposition of Pd onto TiO_2 nanowires for aqueous-phase selective hydrogenation of phenolics to cyclohexanones [J]. Nanoscale, 2020, 12(4).DOI:10.1039/c9nr08324c.
8. Maicu M, Hidalgo MC, G. Colón, et al. Comparative study of the photodeposition of Pt, Au and Pd on pre-sulphated TiO_2 for the photocatalytic decomposition of phenol [J]. Journal of Photochemistry & Photobiology A Chemistry, 2011, 217(2-3):275-283.DOI:10.1016/j.jphotochem.2010.10.020.
9. Tiehu, Wang, Huigang, et.Gold nanoparticle incorporation into nanoporous anatase TiO_2 mesocrystal using a simple deposition-precipitation method for photocatalytic applications [J] . [2025-02-23].
10. Wrasman CJ, Alexey B, Riscoe A R, et al. Synthesis of Colloidal Pd/Au Dilute Alloy Nanocrystals and Their Potential for Selective Catalytic Oxidations [J]. Journal of the American Chemical Society, 2018, 140:jacs.8b07515-.DOI:10.1021/jacs.8b07515.
11. Yun, Zhou, et al. Optimal preparation of Pt/TiO_2 photocatalysts using atomic layer deposition [J]. Applied Catalysis B Environmental, 2010.DOI:10.1016/j.apcatb.2010.09.005.
12. Liu Ping, Wang Xinchen, Fu Xianzhi. Preparation and Characteristics of Photocatalytic Self-cleaning Ceramics [J]. Journal of Inorganic Materials, 2000, 15(1).DOI:10.3321/j.issn:1000-324X.2000.01.015.
13. Qian Hong, Fan Yiqun, Xu Nanping, et al.Preparation of TiO_2 Ecological

Ceramics and Their Antibacterial properties [J]. Journal of Nanjing Tech University (Natural Science Edition), 2001, 23(003):6-9.DOI:10.3969/j.issn.1671-7627.2001.03.002.

14. Xu Ruifen, Xu Xiuyan, Fu Guozhu.Research on the Application Performance of Nano-Titanium Dioxide in Antibacterial Plastics [J]. Plastic, 2002, 31(3):4.DOI:10.3969/j.issn.1001-9456.2002.03.004.
15. Ding Xingeng.Preparation, Performance research and Application of Silver Ion-doped nano-titanium dioxide Powder [D]. Zhejiang University,2002.
16. Xu Ruifen, She Guangwei, Xu Xiuyan.Research on the Degradation of Pollutants and Antibacterial Properties of Nano-tio $_2$ in Composite Coatings [J]. Chemical Industry Exhibition, 2003, 22(11):3.DOI:10.3321/j.issn:1000-6613.2003.11.013.
17. Wang Ming, Ding Xingeng, Cao Xudan, et al.Research on the Preparation of Ag+/TiO_2 Antibacterial Films on Stainless Steel Substrates [J]. Journal of Materials Science and Engineering, 2003, 21(3):4.DOI:10.3969/j.issn.1673-2812.2003.03.017.
18. Lei Yanying, Zhang Xiucheng, Yu Lijun, et al.TResearch on TiO_2 Nano-Microcrystalline Film Sterilized Glass [J]. Architectural Glass and Industrial Glass, 2003(4):3.
19. Wang Chan.Preparation of Nano-Titanium dioxide and Study on Its Photocatalytic Properties [D]. Huazhong University of Science and Technology,2011.
20. Gupta S M , Tripathi M .A review of TiO_2 nanoparticles [J]. Chinese ence

Bulletin, 2011, 56(16):1639.DOI:10.1007/s11434-011-4476-1.

21. Cui Yumin.Factors Affecting the Photocatalytic Activity of Nanomaterial TiO_2 [J]. Rare Metals, 2006(01):107-113.DOI:10.3969/j.issn.0258-7076.2006.01.023.
22. Du Zuojuan. Research on Hydrothermal Preparation and PhotoCatalysis of Nano-Titanium Dioxide [D]. Central South University, 2003. DOI:10.7666/d.y673624.
23. Wang Zhenxing, Ding Shiwen, Zhang Meihong. Synthesis, Structure and Photocatalytic Properties of Highly Dispersed nano-Titanium dioxide Mixed Crystals [J]. Journal of Inorganic Chemistry, 2005(03):147-150.DOI:CNKI:SUN:WJHX.0.2005-03-027.
24. Byrappa K, Adschiri T. Hydrothermal Technology for Nanotechnology [J]. Progress in Crystal Growth and Characterization of Materials, 2007, 53(2):117-166.DOI:10.1016/j.pcrysgrow.2007.04.001.
25. Lim,Jonghun,Lee,et al.Enhanced photocatalytic activity of {101}-oriented bipyramidal TiO_2 agglomerates through interparticle charge transfer [J]. Applied Catalysis, B. Environmental: An International Journal Devoted to Catalytic Science and Its Applications, 2015.
26. Liu J, Yu X, Liu Q, et al.Surface-phase junctions of branched TiO_2 nanorod arrays for efficient photoelectrochemical water splitting [J]. Applied Catalysis B Environmental, 2014, 158-159:296-300.DOI:10.1016/j.apcatb.2014.04.032.
27. Xu H, Li G, Zhu G, et al. Enhanced photocatalytic degradation of rutile/anatase TiO_2 heterojunction nanoflowers [J]. Catalysis Communications, 2015,

62:52-56.DOI:10.1016/j.catcom.2015.01.001.

28. Li S, Li N, Li G, et al. Protonated titanate nanotubes as a highly active catalyst for the synthesis of renewable diesel and jet fuel range alkanes [J]. Applied Catalysis B Environmental, 2015, 170-171:124-134.DOI:10.1016/j.apcatb.2015.01.022.
29. Zoltán Győri, Zoltán Kónya, Ákos Kukovecz. Visible light activation photocatalytic performance of PbSe quantum dot sensitized TiO_2 Nanowires [J]. Applied Catalysis B: Environmental, 2015.DOI:10.1016/j.apcatb.2015.05.056.
30. Wu H, Fan J, Liu E, et al. Facile hydrothermal synthesis of TiO_2 nanospindles-reduced graphene oxide composite with a enhanced photocatalytic activity [J]. Journal of Alloys and Compounds, 2015.DOI:10.1016/j.jallcom.2014.10.153.
31. Wang H, Cao S, Cen C, et al. Structure–Activity Relationship of Titanate Nanotube-Confined Ceria Catalysts in Selective Catalytic Reduction of NO with Ammonia [J]. Catalysis Letters, 2013, 143(12):1312-1318.DOI:10.1007/s10562-013-1084-5.
32. Erjavec, Boštjan, Kaplan, et al. Effects of heat and peroxide treatment on photocatalytic activity of titanate nanotubes. [J]. Catalysis Today, 2015.
33. Erjavec B, Kaplan R, Pintar A. Effects of heat and peroxide treatment on photocatalytic activity of titanate nanotubes [J]. Catalysis Today, 2015, 241:15-24.DOI:10.1016/j.cattod.2014.04.005.
34. AKHS, AHBK, BHSK, et al. Impact of area under the concentration–time

curve to minimum inhibitory concentration ratio on vancomycin treatment outcomes in methicillin-resistant Staphylococcus aureus bacteraemia [J]. International Journal of Antimicrobial Agents, 2015, 46(6):689-695.DOI:10.1016/j.ijantimicag.2015.09.010.

35. Chen S, Guo Y, Chen S, et al. Fabrication of Cu/TiO_2 nanocomposite: Toward an enhanced antibacterial performance in the absence of light [J]. Materials Letters, 2012, 83:154-157.DOI:10.1016/j.matlet.2012.06.007.
36. Chen S, Guo Y, Chen S, et al. Facile preparation and synergistic antibacterial effect of three-component Cu/TiO2/CS nanoparticles [J]. Journal of Materials Chemistry, 2012, 22(18):9092.DOI:10.1039/C2JM00063F.
37. Dumitriu C, Ungureanu C, Popescu S, et al. Ti surface modification with a natural antioxidant and antimicrobial agent [J]. Surface & Coatings Technology, 2015. DOI:10.1016/j.surfcoat.2015.06.063
38. Erjavec, Bostjan, Kaplan, et al. Enhanced photocatalytic activity of single-phase, nanocomposite and physically mixed TiO2 polymorphs [J]. Applied Catalysis, A. General: An International Journal Devoted to Catalytic Science and Its Applications, 2015, 489:51-60.
39. Limmer SJ, Seraji S, Wu Y, et al.T emplate-Based Growth of Various Oxide Nanorods by Sol–Gel Electrophoresis [J]. Advanced Functional Materials, 2002, 12(1):59–64. DOI:10.1002/1616-3028(20020101)12:13.0.CO;2-B.
40. Xiaoyun Li, Guanhui Gao, Chengjun Sun. Preparation and antibacterial performance testing of Ag nanoparticles embedded biological materials [J]. Applied Surface Science, 2015. DOI:10.1016/j.apsusc.2015.01.004.

41. Anitha, V. C, Joo, et al. Recent developments in TiO_2 as n- and p-type transparent semiconductors: synthesis, modification, properties, and energy-related applications [J]. Journal of Materials Science, 2015.

42. Anitha, V. C, Joo, et al. Recent developments in TiO2 as n- and p-type transparent semiconductors: synthesis, modification, properties, and energy-related applications [J]. Journal of Materials Science, 2015.

43. Calogero G, Citro I, Crupi C, et al. Absorption spectra and photovoltaic characterization of chlorophyllins as sensitizers for dye-sensitized solar cells[J].Spectrochimica Acta Part A Molecular & Biomolecular Spectroscopy, 2014, 132:477-484. DOI:10.1016/j.saa.2014.04.196.

44. Roy MS, Balraju P, Kumar M, et al. Dye-sensitized solar cell based on Rose Bengal dye and nanocrystalline TiO_2 [J]. Solar Energy Materials and Solar Cells, 2008, 92(8):909-913. DOI:10.1016/j.solmat.2008.02.022.

45. Yotsumoto Neto S, Luz, Rita de Cássia Silva, Damos, Flávio Santos.Visible LED light photoelectrochemical sensor for detection of L-Dopa based on oxygen reduction on TiO_2 sensitized with iron phthalocyanine [J]. Electrochemistry Communications, 2016, 62:1-4.DOI:10.1016/j.elecom.2015.10.018.

46. Mu Oz-Batista MJ, Ferrer M, Fernández-García, Marcos, et al. Abatement of organics and Escherichia coli using CeO_2-TiO_2 composite oxides: Ultraviolet and visible light performances [J]. Applied Catalysis B Environmental, 2014, 154-155:350-359. DOI:10.1016/j.apcatb.2014.02.038.

47. Dhanalakshmi R, Pandikumar A, Sujatha K, et al. Photocatalytic and

antimicrobial activities of functionalized silicate sol–gel embedded ZnO–TiO_2 nanocomposite materials [J]. Materials Express, 2013, 3(4):291-300. DOI:10.1166/mex.2013.1133.

48. Nishikawa M, Takanami R, Nakagoshi F, et al. Dominated factors for high performance of Fe3+ grafted metal doped TiO_2 based photocatalysts [J]. Applied Catalysis B Environmental, 2014, 160-161:722-729. DOI:10.1016/j.apcatb.2014.05.020.
49. Pelaez M, Nolan NT, Pillai SC, et al. A review on the visible light active titanium dioxide photocatalysts for environmental applications [J]. Applied Catalysis B: Environmental, 2012. DOI:10.1016/j.apcatb.2012.05.036.
50. Zhang Z , Yates JT. ChemInform Abstract: Band Bending in Semiconductors: Chemical and Physical Consequences at Surfaces and Interfaces [J]. Chemical Reviews, 2012, 112(10):5520-5551. DOI:10.1021/cr3000626.